Ru-σ-alkynyl compounds of tetraanilinopyridinato-diruthenium(II,III) core: synthesis and structural characterization

Gang Zou, Julio C. Alvarez, Tong Ren *

Department of Chemistry, University of Miami, PO Box 249118, Coral Gables, FL 33124-0431, USA

Dedicated to Professor F. Albert Cotton on the occasion of his 70th birthday

Abstract

Synthesis and characterizations are reported for three diruthenium(II,III) compounds of general formula $Ru_2(ap)_4(C\equiv CR)$, where ap = 2-anilinopyridinate and R = $Si(CH_3)_3$ (**3**), H (**4**), and CH_2OCH_3 (**5**). Molecular structure determination reveals that the Ru–Ru bond lengths are 2.3162(5) and 2.3234(7) Å for **3** and **5**, respectively, while the $C\equiv C$ bond is not significantly elongated compared with the free alkyne. Compounds **3–5** undergo reversible one-electron oxidation and reduction at potentials around 200 and −1030 mV, respectively. At more positive potential, compounds **3** and **4** undergo the second one-electron oxidation quasireversibly or irreversibly without decomposition, while compound **5** is oxidatively degraded. © 2000 Elsevier Science S.A. All rights reserved.

Keywords: Diruthenium compounds; Alkynyl; 2-Anilinopyridinate; Electrochemistry

1. Introduction

Study of paddlewheel species bearing axial alkynyl ligands was pioneered by Chakravarty and Cotton, who prepared $Ru_2(ap)_4(C\equiv CPh)$ (**2**, ap = 2-anilinopyridinate), the first paddlewheel species with an organometallic axial ligand other than carbon monoxide, from the reaction between $Ru_2(ap)_4Cl$ (**1**) and $LiC\equiv CPh$ [1]. Subsequent studies from Bear's group demonstrated that dirhodium and diruthenium compounds supported by 2-anilinopyridinate, 2-pentafluoroanilinopyridinate, and diphenylformamidinate ligands are capable of forming both mono- and bis-axial alkynyl adducts [2–5]. Compounds of general formula $Ru_2(ArNC(H)NAr)_4(C\equiv CPh)_m$ with $m = 1, 2$ and Ar as the phenyl substituted with either p-MeO, or p-(m-)Cl, or p-(m-)CF_3, or 3,4-Cl_2, or 3,5-Cl_2 were prepared in our laboratory [6,7], where electronic perturbation due to the phenyl substituent was explored.

Both Bear's and our work revealed that these dinuclear species are rich in electrochemistry and most of them can be reversibly one-electron reduced and oxidized. Presence of reversible one-electron reduction renders the intermediate **A** in Scheme 1 accessible, which, in the presence of electrophile E^+ (H^+ or R^+), may be converted to a dinuclear species bearing axial vinylidene (**B**), an elusive target we have pursued for years.

Since axial vinylidene ligand is sterically bulkier than axial alkynyl, compounds of general formula $Ru_2(ArNC(H)NAr)_4(C\equiv CPh)_m$ may not be suitable as the starting materials in the route outlined in Scheme 1. To maximize the space around the alkynyl ligand, we decided to explore the possibility of using compounds of general formula $Ru_2(ap)_4(C\equiv CR)$ as the starting materials, where, as demonstrated by Cotton and Chakravarty [1], the bridging 2-anilinopyridinates adopt (4,0)-arrangement with all four phenyl rings on the opposite site of axial alkynyl ligand. From common starting material $Ru_2(ap)_4Cl$ (**1**), three new compounds of formula $Ru_2(ap)_4(C\equiv CR)$ with R = $Si(CH_3)_3$ (**3**), H (**4**), and CH_2OCH_3 (**5**) have been synthesized, and

* Corresponding author. Fax: + 1-305-2841880.
E-mail address: tren@miami.edu (T. Ren).
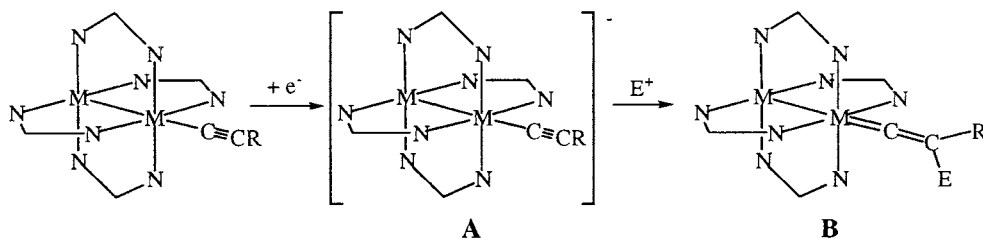
Scheme 1. Possible synthetic route to axial vinylidene.

characterized with X-ray diffraction, UV–vis and IR spectroscopy, and cyclic voltammetry.

2. Results and discussion

2.1. Synthesis

Analogously to $Ru_2(ap)_4(C{\equiv}CPh)$ [1], compounds **3** and **5** were prepared by reacting $Ru_2(ap)_4Cl$ (**1**) with $LiC{\equiv}CSi(CH_3)_3$ and $LiC{\equiv}CCH_2OCH_3$ salts, respec-

Fig. 1. The ORTEP plot of compound **3** at the 20% probability level.

Fig. 2. The ORTEP plot of compound **5** at the 20% probability level.

tively. Compound **4** was readily obtained by treating **3** with standard desilylation reagent Bu_4NF [8]. Compounds **3**–**5** were purified with silica gel flash column chromatography. Similar to our earlier experience with $Ru_2(ArNC(H)NAr)_4(C{\equiv}CPh)_m$ compounds [6,7], compounds **3**–**5** are susceptible to thermal decomposition when heated above 45°C, which prevents a complete removal of solvent in the samples submitted for analysis (**3** and **5**). Earlier preparation of **1** in a good yield of 73% involves small scale molten reaction between $Ru_2(OAc)_4Cl$ (0.2 mmol) and 2-anilinopyridine [9]. An alternative route involving base-assisted ligand metathesis (see Section 3.1) is adapted to provide **2** in quantitative yield. This technique was developed by Doyle et al. for the synthesis of $Rh_2(carboxamidate)_4$ [10], and may become a convenient high-yield route for other dinuclear species, as evidenced by our success.

2.2. Molecular and electronic structures

Overall features of the molecular structures of **3** and **5**, shown respectively in Figs. 1 and 2, are very similar to that of $Ru_2(ap)_4(C{\equiv}CPh)$ [1]. As anticipated, four 2-anilinopyridinate ligands are in the polar (4,0) arrangement around the diruthenium(II,III) core. The Ru(II)–Ru(III) bond lengths are 2.3162(5) and 2.3234(7) Å for **3** and **5**, respectively, which are statistically identical to that of $Ru_2(ap)_4(C{\equiv}CPh)$ (2.319(3) Å) and significantly longer than that of $Ru_2(ap)_4Cl$ (2.275(3) Å). Elongation of the Ru(II)–Ru(III) bond upon replacing the axial chloro ligand with alkynyl is likely due to the strong Lewis-base nature of the latter, which commands a strong σ(Ru–C) bond at the expense of a σ(Ru–Ru) bond. The averaged Ru(II)–N and Ru(III)–N distances are 2.046(2) and 2.096(2) Å in **3**, and 2.035(5) and 2.095(5) Å in **5**. A longer Ru(III)–N bond compared with Ru(II)–N is clearly attributed to the steric effect of axial C≡CR ligands, since an opposite order would be anticipated if only the formal oxidation state and covalent radius are considered. The averaged torsional angles N–Ru–Ru′–N′ in **3** and **5** are 20.3 and 16.2°, respectively, which are comparable to those of $Ru_2(ap)_4(C{\equiv}CPh)$ (19.5°) and $Ru_2(ap)_4Cl$ (22.7°). Other significant metric parameters for both **3** and **5** are summarized in Table 1.

Table 1
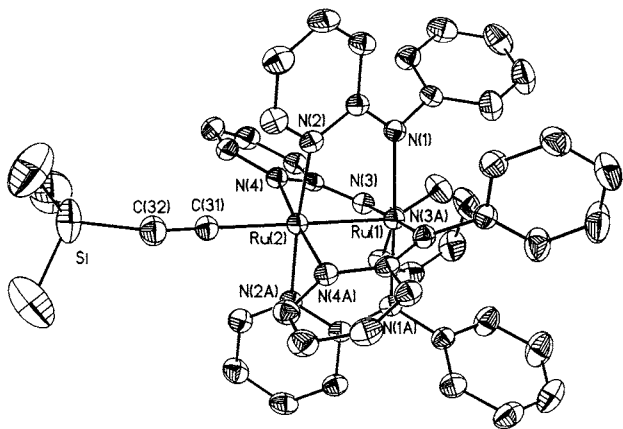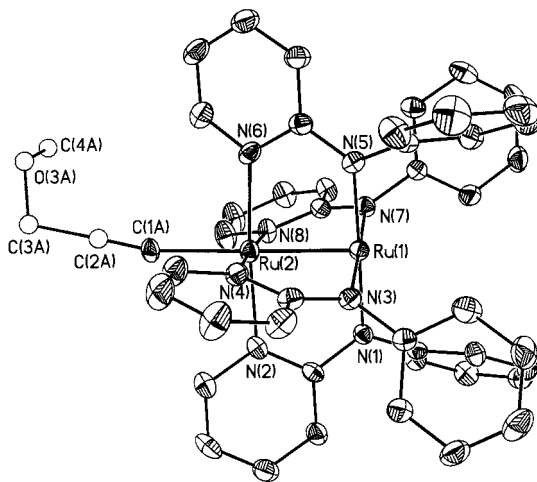Selected bond lengths (Å) and angles (°) for molecules **3** and **5**

3		**5**	
Bond lengths			
Ru(1)–Ru(2)	2.3162(5)	Ru(1)–Ru(2)	2.3234(7)
Ru(1)–N(1)	2.043(2)	Ru(1)–N(1)	2.033(4)
Ru(2)–N(2)	2.098(2)	Ru(1)–N(3)	2.033(5)
Ru(1)–N(3)	2.049(2)	Ru(1)–N(5)	2.044(5)
Ru(2)–N(4)	2.094(2)	Ru(1)–N(7)	2.029(5)
Ru(2)–C(31)	2.077(4)	Ru(2)–N(2)	2.098(5)
C(31)–C(32)	1.207(6)	Ru(2)–N(4)	2.097(5)
Si–C(32)	1.834(5)	Ru(2)–N(6)	2.090(5)
		Ru(2)–N(8)	2.094(5)
		Ru(2)–C(1A)	2.139(7)
		C(1A)–C(2A)	1.144(16)
		C(2A)–C(3A)	1.57(2)
Bond angles			
N(1)–Ru(1)–Ru(2)	89.09(6)	N(1)–Ru(1)–Ru(2)	89.55(13)
N(3)–Ru(1)–Ru(2)	88.71(6)	N(3)–Ru(1)–Ru(2)	89.59(14)
N(2)–Ru(2)–Ru(1)	87.59(6)	N(5)–Ru(1)–Ru(2)	89.57(15)
N(4)–Ru(2)–Ru(1)	88.00(6)	N(7)–Ru(1)–Ru(2)	89.44(14)
C(31)–Ru(2)–Ru(1)	180.0	N(2)–Ru(2)–Ru(1)	87.71(14)
C(32)–C(31)–Ru(2)	180.0	N(4)–Ru(2)–Ru(1)	88.07(15)
C(31)–C(32)–Si	161.97(10)	N(6)–Ru(2)–Ru(1)	87.71(14)
		N(8)–Ru(2)–Ru(1)	88.05(14)
		C(1A)–Ru(2)–Ru(1)	179.0(2)
		C(2A)–C(1A)–Ru(2)	167(3)
		C(1A)–C(2A)–C(3A)	173(5)
N(2)–Ru(2)–Ru(1)–N(1)	20.29(10)	N(1)–Ru(1)–Ru(2)–N(2)	16.32(18)
N(4)–Ru(2)–Ru(1)–N(3)	20.31(9)	N(3)–Ru(1)–Ru(2)–N(4)	15.60(18)
		N(5)–Ru(1)–Ru(2)–N(6)	17.05(19)
		N(7)–Ru(1)–Ru(2)–N(8)	15.86(19)

There has been substantial interest in probing the nature of the M–C≡C interaction through examining both the M–C and C≡C bond lengths [11]. In molecule **3**, the Ru–C distance (2.077(4) Å) is the same as that of Ru$_2$(ap)$_4$(C≡CPh) (2.08(3) Å) [1], and slightly longer than those found in Ru$_2$(ArNC(H)NAr)$_4$(C≡CPh) (2.02–2.06 Å) [4,7]. The relative constancy of Ru–C bond length among the above-mentioned diruthenium mono-alkynyl compounds is indicative of the absence of significant M–C≡C π-interaction, either back-donation or filled–filled type [11]. The C≡C bond length in **3**, 1.207(6) Å, is very close to the mean of known trimethylsilylethynyl complexes (1.210(13) Å) [11], and slightly longer than those of diruthenium phenylethynyl compounds (1.14–1.197 Å) [1,7]. Although similar Ru–C and C≡C bond lengths have been obtained for molecule **5**, meaningful comparison cannot be made due to the severe disorder of the C≡C–CH$_2$OCH$_3$ group.

Two intense absorptions in the visible region were recorded at 746 and 470 nm for **3**, 749 and 466 nm for **4**, 747 and 467 nm for **5**, and these λ_{max} values are comparable to those of Ru$_2$(ap)$_4$(C≡CPh) (735 and 480 nm). Both transitions are tentatively assigned as the ligand-to-metal charge transfer transitions (π(C≡C) →

π*/δ*(Ru–Ru)). Spectral similarity among these diruthenium monoalkynyl complexes clearly indicates that they are isoelectronic. Based on the assumption that the lowest energy absorption corresponds to the HOMO–LUMO transition, the optical HOMO–LUMO gap has been calculated and listed in Table 2. Identical HOMO–LUMO gaps (ca. 1.66 eV) were found for new compounds **3–5**. Effective magnetic moments obtained at room temperature are 3.93, 4.09, and 4.02 Bohr magneton for **3**, **4**, and **5**, respectively, which are consistent with a $S = 3/2$ ground state. Based on the studies of other diruthenium(II,III) systems [7,12,13], the ground-state configuration for Ru$_2$(ap)$_4$-(C≡CR) species is $\sigma^2\pi^4\delta^2(\pi^*\delta^*)^3$, and the formal Ru–Ru bond order is 2.5.

2.3. Electrochemistry

As stated in Section 1, we are particularly interested in the redox properties of Ru$_2$(ap)$_4$(C≡CR) species, which were examined via the cyclic voltammetry measurement, and the relevant data are listed in Table 2. Cyclic voltammograms of known compounds **1** and **2** were also measured to ensure that all the data to be compared were obtained under the same experimental

Table 2
Electrochemical optical data for $Ru_2(ap)_4(C\equiv CR)$ and $Ru_2(ap)_4Cl$ [a]

	1 [b]	2 [b]	3	4	5
$E_{1/2}(Ru_2^{5+/4+})$ (mV)	−834	−1036	−1021	−1026	−1046
$(\Delta E_p, i_{p,c}/i_{p,a})$	(70, 1.14)	(60, 0.91)	(58, 0.92)	(58, 1.06)	(58, 1.04)
$E_{1/2}(Ru_2^{6+/5+})$ (mV)	457	187	197	199	196
$(\Delta E_p, i_{p,a}/i_{p,c})$	(73, 0.99)	(58,1.13)	(59, 1.04)	(59, 1.04)	(58, 1.06)
$E_{pa}(Ru_2^{7+/6+})$ (mV)	1430	–	–	1297	–
$E_{1/2}(Ru_2^{7+/6+})$ (mV)	–	–	1264	–	–
$(\Delta E_p, i_{p,a}/i_{p,c})$	–	–	(129, 1.70)	–	–
$\Delta E_{1/2}$ (mV) [c]	1291	1223	1218	1225	1242
E_{op} (eV) [d]	1.623	1.687	1.662	1.655	1.660

[a] All data were recorded in 0.1 M $(n$-Bu$)_4NPF_6$ solution (CH$_2$Cl$_2$, N$_2$-degassed) with a glassy carbon working, a Pt-wire auxiliary electrodes, and an Ag|AgCl reference electrode; [Ru$_2$] = 1.0 mM.

[b] Electrochemical data reported initially in references [1,17], but re-measured in this work to ensure the consistency. λ_{max} were taken directly from the original references [1,9].

[c] $\Delta E_{1/2} = E_{1/2}$ (Ru$_2^{6+/5+}$) − $E_{1/2}$ (Ru$_2^{5+/4+}$).

[d] $E_{op} = 10^7/(8065.5\lambda_{max(HOMO-LUMO)})$.

condition. As shown in Fig. 3, known compound **2** and new compounds **3–5** undergo two one-electron processes when the potential sweeping range is limited to $\leq +600$ mV: a reduction (Ru$_2^{5+} \rightarrow$ Ru$_2^{4+}$) around -1030 mV and an oxidation (Ru$_2^{5+} \rightarrow$ Ru$_2^{6+}$) around $+190$ mV. Judged from both the ΔE_p values and the $i_{forward}/i_{backward}$ ratio, these redox couples are highly reversible. However, small post-wave peaks are present for both the first oxidation of **2** and the reduction of **4**, indicating possible adsorption on the electrode surface by the unoxidized (or unreduced) species. Compared with the parent compound Ru$_2$(ap)$_4$Cl, the reduction (Ru$_2^{5+/4+}$) and oxidation (Ru$_2^{6+/5+}$) potentials of Ru$_2$(ap)$_4$(C≡CR) have been cathodically shifted ca. 200 and 260 mV, respectively. The cathodic shift in electrode potentials reflects the destabilization of both the HOMO and LUMO due to the strong nucleophilicity of alkynyl ligand, as discussed earlier for Ru$_2$-(ArNC(H)NAr)$_4$(C≡CR) [6,7].

Since both reduction (Ru$_2^{5+/4+}$) and oxidation (Ru$_2^{6+/5+}$) couples are reversible and their $E_{1/2}$ values are accurately determined, the electrochemical HOMO–LUMO gap can be calculated via the following relationship [14,15]:

$$E_{1/2}(Ru_2^{6+/5+}) - E_{1/2}(Ru_2^{5+/4+})$$
$$= E(LUMO) - E(HOMO) \quad (1)$$

where both the E(LUMO) and E(HOMO) refer to the solvated molecule. The electrochemical HOMO–LUMO gaps for compounds **2–5**, listed in Table 2, are in a narrow range of 1218–1242 mV, and significantly lower than the corresponding optical HOMO–LUMO gap (E_{op} in eV). Two HOMO–LUMO gaps are related theoretically by the following equation [14]:

$$E_{op} = [E_{1/2}(oxidation) - E_{1/2}(reduction)] - J_{12} + 2K_{12} \quad (2)$$

where J_{12} and K_{12} are the Coulomb repulsion and exchange integrals, respectively. Our result thus convincingly demonstrates that the '$-J_{12} + 2K_{12}$' term, ca. 0.4 eV, is very positive for diruthenium species.

While compounds **2–5** show nearly identical redox activity in the negative to mildly positive potential window, great disparity has been found in their behaviors at more positive potentials. When scanned between $+600$ and $+1500$ mV, compound **3** displays an anodic wave (ca. 1260 mV) with an apparent shoulder. The presence of two electron-transfer events was revealed by the measurement of Osteryoung square-wave voltam-
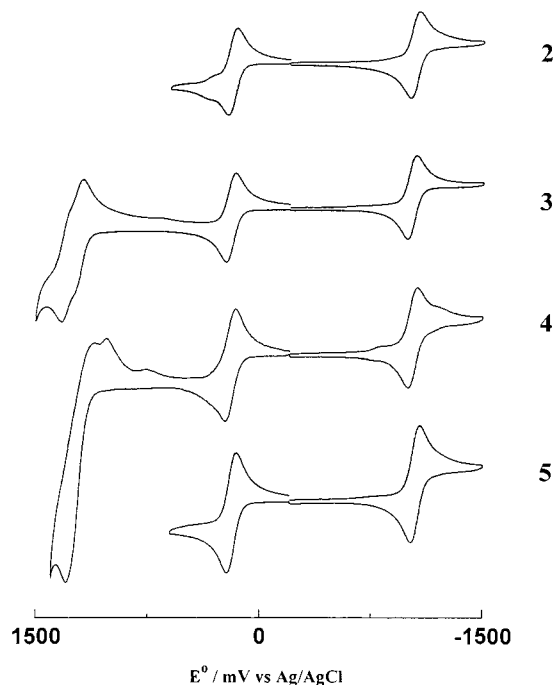

Fig. 3. Cyclic voltammograms of compounds **2–5** recorded in CH$_2$Cl$_2$ with a scan rate of 100 mV s^{-1}.
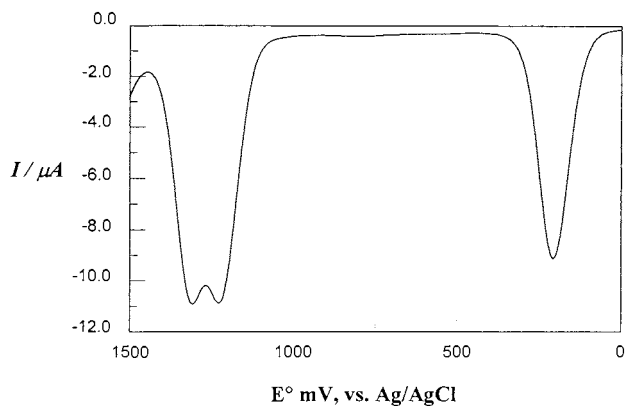
Fig. 4. Osteryoung square-wave voltammogram for the oxidation of compound **3** ([**3**] = 1.0 mM, 0.2 M Bu$_4$NPF$_6$ in CH$_2$Cl$_2$ versus Ag|AgCl).

metry [16], as shown in Fig. 4. Although it is still unclear if two waves are coupled, both of them are electrochemically reversible. Repeated scan in this potential range yielded the identical cyclic voltammogram, suggesting the absence of chemical decomposition of **3** upon the oxidation.

Compound **4**, the desilylation product of **3**, displays a huge anodic peak around 1300 mV and a greatly suppressed cathodic wave which is split into several small peaks. This behavior is consistent with a multi-step process involving fragmentation of electroactive groups, although further investigation is needed to unravel the mechanistic details. Nevertheless, the voltammetric response is also reproducible under continuous scanning.

In contrast, no well-defined anodic/cathodic waves can be located for either **2** or **5** when scanned between + 600 and 1500 mV. Furthermore, the whole anodic response is severely distorted after the first scan above 600 mV and consists of new peaks characteristic of electrode surface adsorption. In order to recover the initial cyclic voltammogram, the working electrode has to be polished. The observed voltammetric irreproducibility, consistent with the earlier study of **2** [1], clearly indicates that both **2** and **5** are highly susceptible to oxidative degradation. Since the oxidatively stable (**3** and **4**) and unstable (**2** and **5**) species differ in the absence/presence of γ-carbon (α- and β-carbons belong to ethynyl group), the degradation pathway likely involves chemical coupling at γ-carbon center instead of the cleavage of Ru–C bond.

3. Experimental

3.1. Starting materials and instruments

Methyl propargyl ether and 2-anilinopyridine were purchased from Aldrich, NBu$_4$F–THF and trimethylsi-

lylacetylene from ACROS, and silica gel (SIP® Brand 60 Å, 230–400 mesh) from Baxter. Ru$_2$(OAc)$_4$Cl [18] and Ru$_2$(ap)$_4$(C≡CPh) [1] were prepared according to the literature. THF, hexanes, and toluene were distilled over Na–benzophenone under a N$_2$ atmosphere prior to use. Infrared spectra were recorded on a Perkin–Elmer Paragon 1000 FTIR spectrometer using KBr disks. UV–vis spectral data (in CH$_2$Cl$_2$) were obtained with a Shimadazu UV-2101PC UV–vis spectrophotometer. Magnetic susceptibilities were measured at 293 K with a Johnson Matthey Mark-I Magnetic Susceptibility Balance. Elemental analysis was performed by Atlantic Microlab, Norcross, GA. Cyclic voltammograms were recorded in 0.1 M (*n*-Bu)$_4$NPF$_6$ solution (CH$_2$Cl$_2$, N$_2$-degassed) on a BAS CV-100 W voltammetric analyzer with a glassy carbon working electrode, a Pt-wire auxiliary electrodes, and an Ag|AgCl reference electrode. The concentration of diruthenium species is always 1.0 mM. Osteryoung square-wave voltammetry was performed with the same solution and electrode system as for the CV experiments. The potential step applied was 4 mV with a square-wave frequency of 15 Hz, which resulted in a scan rate of 60 mV s^{-1}.

3.2. Synthesis of Ru$_2$(ap)$_4$Cl (**1**)

A round-bottom flask was charged with Ru$_2$-(OAc)$_4$Cl (0.474 g, 1.00 mmol), 2-anilinopyridine (1.70 g, 10 mmol) and 40 ml of toluene, and to which a micro Soxhlet apparatus with a glass thimble filled with the mixture of sand (3 g) and K$_2$CO$_3$ (2 g) was mounted. The mixture was gently refluxed in ambient atmosphere for 4 days. Toluene was removal by distillation and the residue was extracted with 40 ml of CH$_2$Cl$_2$ and filtered. The volume of the filtrate was reduced to 5 ml and 60 ml of warm (ca. 50°C) MeOH was added. After standing at ambient temperature overnight, the green microcrystalline product was collected by filtration and dried under the vacuum. The product was authenticated by a TLC test (CH$_2$Cl$_2$–hexanes–Et$_3$N, 9:1:0.1, v/v/v) against a sample prepared by the original molten reaction method [9]. Yield: 0.905 g (99% based on Ru).

3.3. Synthesis of Ru$_2$(ap)$_4$(C≡CSiMe$_3$) (**3**)

To a 20 ml THF solution containing 3.0 mmol HC≡CSiMe$_3$ was added 2.0 ml BuLi (1.6 M in hexanes) at about −50°C. The mixture was stirred for 1 h at −50°C before being warmed to room temperature (r.t.) to yield a colorless clear solution. A 3.0 ml portion of the solution was added to a THF (15 ml) solution of Ru$_2$(ap)$_4$Cl (0.184 g, 0.2 mmol) at 0°C (ice-bath) and the mixture was stirred for 3 h. Removal of solvent in vacuum yielded a green powder, which was purified by

flash column chromatography on silica gel deactivated by 10% NEt$_3$ in hexanes with eluent ethyl acetate–hexanes (3:8, v/v). Yield: 0.178 g (89% based on Ru). Anal. Calc. (Found) for **3**·0.5C$_6$H$_{14}$ (C$_{52}$H$_{52}$N$_8$SiRu$_2$): C, 61.28 (61.38); H, 5.14 (4.93); N, 10.99 (11.22). UV–vis in CH$_2$Cl$_2$ (λ, nm (ε, M^{-1} cm^{-1})): 746 (9644), 470 (13 165), 325 (sh) and 253 (sh). IR (cm^{-1}): ν(C≡C), 1994. χ_{mol}(corrected) = 6.62 × 10^{-3} emu, μ_{eff} = 3.93 BM.

3.4. Synthesis of Ru$_2$(ap)$_4$(C≡CH) (4)

Ru$_2$(ap)$_4$(C≡CSiMe$_3$) (98 mg, 0.10 mmol) was dissolved in 20 ml of THF, to which 1.0 ml of Bu$_4$NF in THF (1.0 M) was added. The mixture was stirred at r.t. until the complete consumption of the starting material indicated by TLC (5 days). Green crude product was obtained upon the removal of solvent, which was purified by flash column chromatography under the same condition as that of **3** to yield 60 mg analytically pure product (65%). Anal. Calc. (Found) for **4** (C$_{46}$H$_{37}$N$_8$Ru$_2$): C, 61.12 (61.29); H, 4.13 (4.20); N, 12.40 (12.24). UV–vis in CH$_2$Cl$_2$ (λ, nm (ε, M^{-1} cm^{-1})): 749 (7048), 466 (8378), 325 (sh) and 253 (sh). IR (cm^{-1}): ν(C≡**C**–**H**), 3259; ν(C≡C), 1951. χ_{mol}(corrected) = 7.13 × 10^{-3} emu, μ_{eff} = 4.09 BM.

3.5. Synthesis of Ru$_2$(ap)$_4$(C≡CCH$_2$OCH$_3$) (5)

This compound was prepared similarly to **3**. Ru$_2$-(ap)$_4$Cl (94 mg, 0.10 mmol) was reacted with LiC≡CCH$_2$OMe (prepared in situ from 0.24 mmol methyl propargyl ether and 0.15 ml of 1.6 M BuLi) at 0°C for 3 h. Crude product was purified by flash column chromatography on silica gel deactivated by 10% NEt$_3$ in hexanes with a linear gradient of ethyl acetate–hexanes (from 2:8 to 4:8, v/v). Further recrystallization from diethyl ether yielded 74 mg green needles (78% based on Ru). Anal. Calc. (Found) for **5**·0.5C$_6$H$_{14}$ (C$_{51}$H$_{48}$N$_8$ORu$_2$): C, 61.80 (61.99); H, 5.36 (5.16); N, 11.30 (10.85). UV–vis in CH$_2$Cl$_2$ (λ, nm (ε, M^{-1} cm^{-1})): 747 (5184), 467 (6633), 327 (sh) and 253 (sh). IR (cm^{-1}): ν(C≡C), 1945. χ_{mol}(corrected) = 6.90 × 10^{-3} emu, μ_{eff} = 4.02 BM.

3.6. X-ray data collection, processing, and structure analysis and refinement

Dark green thin plates were grown via slow diffusion of hexanes into either a THF solution (**3**) or a CH$_2$Cl$_2$ solution (**5**). The X-ray intensity data were measured at 300 K on a Bruker SMART1000 CCD-based X-ray diffractometer system equipped with a Mo-target X-ray tube (0.71073 Å) operated at 2000 W power. Data sets were collected using omega scans of 0.3° per frame for 10 s such that a hemisphere was collected. A total of

1271 frames was collected with a final resolution of 0.75 Å. No decay was indicated by the recollection of the first 50 frames at the end of data collection for either crystal. The frames were integrated with the Bruker SAINT© software package [19] using a narrow-frame integration algorithm, which also corrects for the Lorentz and polarization effects. Absorption corrections were applied using SADABS supplied by George Sheldrick. Structural solution and refinement were performed within the Bruker SHELXTL© (Version 5.1) Software Package [20–22].

For the structure of **3**, the direct method revealed all non-hydrogen atoms. Both ruthenium atoms and acetylenic carbon atoms are located on a crystallographic twofold axis of the space group C2/c. The asymmetric unit contains one half of the diruthenium molecule, which is related to the other half through the

Table 3
Crystal data for compounds **3** and **5**·*n*-C$_6$H$_{14}$

	3	**5**·*n*-C$_6$H$_{14}$
Formula	C$_{49}$H$_{45}$N$_8$SiRu$_2$	C$_{54}$H$_{55}$N$_8$ORu$_2$
Formula weight	980.15	1034.20
Crystal system	Monoclinic	Triclinic
Space group	C2/c	P$\bar{1}$
a (Å)	14.0085(14)	10.0597(6)
b (Å)	25.155(2)	13.7001(8)
c (Å)	13.7806(14)	18.2760(11)
α (°)	90	98.883(2)
β (°)	90.733(2)	94.828(2)
γ (°)	90	92.442(2)
Volume (Å^3)	4855.7(8)	2475.8(3)
Z	4	2
ρcalc (g cm^{-3})	1.335	1.387
μ (mm^{-1})	0.687	0.656
λ(Mo–K$_\alpha$) (Å)	0.71073	0.71073
F(000)	1988	1062
Crystal size (mm)	0.35 × 0.30 × 0.03	0.33 × 0.22 × 0.02
θ range (°)	1.62–25.00	1.51–25.00
Index ranges	−16 ≤ h ≤ 14, −22 ≤ k ≤ 29, −11 ≤ l ≤ 16	−11 ≤ h ≤ 11, −10 ≤ k ≤ 16, −21 ≤ l ≤ 21
Reflections collected	12 747	13 159
Independent reflections	4277 [R$_{int}$ = 0.0242]	8608 [R$_{int}$ = 0.0267]
Refinement method	Full-matrix least-squares on F2	Full-matrix least-squares on F^2
Data/restraints/ parameters	4277/0/290	8608/103/593
Instrument	SMART1000 CCD	SMART1000 CCD
T (K)	300(2)	300(2)
Final R indices (I > 2σ(I))	R$_1$ = 0.0287, wR$_2$ = 0.0748	R$_1$ = 0.0531, wR$_2$ = 0.1392
R indices (all data)	R$_1$ = 0.0474, wR$_2$ = 0.0848	R$_1$ = 0.0866, wR$_2$ = 0.1595
Goodness-of-fit on F^2 [a]	0.986	0.980
Largest difference peak and hole (e Å^{-3})	0.918 and −0.368	0.663 and −0.936

[a] Goodness-of-fit = [$\Sigma[w(F_o^2 - F_c^2)^2] = (n-p)$]$^{1/2}$.

twofold rotation. Although the initial solution of direct method suggested that the Si atom was also situated on the twofold axis, the structure refines much better with the Si atom (0.5 occupancy) in a general position close to the twofold axis. With all non-hydrogen atoms being anisotropic and all hydrogen atoms in calculated position and riding mode the structure was refined to convergence by least squares method on F^2, SHELXL-93 [20,21], incorporated in the Bruker SHELXTL© (Version 5.1) Software Package [22].

For the structure of **5**, both direct and Patterson methods failed to provide an initial solution in the space group $P\bar{1}$. Instead, positions of the ruthenium atoms were determined using Patterson method in the space group $P1$ and then refined in the space group $P\bar{1}$. The remaining non-hydrogen atoms were introduced through alternating least-squares refinement and difference Fourier analysis. Although most of non-hydrogen atoms were refined well, both the axial ligand $C{\equiv}CCH_2OCH_3$ and a lattice hexane solvent were severely disordered and each was refined as the sum of three disordered fragments under geometrical restraints (Table 3).

4. Supplementary material

Crystallographic data have been deposited with the Cambridge Crystallographic Data Centre as CCDC nos. 135662 and 135926 for compounds **3** and **5**, respectively. Copies of this information may be obtained free of charge from The Director, CCDC, 12 Union Road, Cambridge, CB2 1EZ, UK (Fax: +44-1223-336033; e-mail: deposit@ccdc.cam.ac.uk or www: http://www.ccdc.cam.ac.uk).

References

[1] A.R. Chakravarty, F.A. Cotton, Inorg. Chim. Acta 113 (1986) 19.
[2] J.L. Bear, B. Han, S. Huang, J. Am. Chem. Soc. 115 (1993) 1175.
[3] C.-L. Yao, K.H. Park, A.R. Khokhar, M.-J. Jun, J.L. Bear, Inorg. Chem. 29 (1990) 4033.
[4] J.L. Bear, B. Han, S. Huang, K.M. Kadish, Inorg. Chem. 35 (1996) 3012.
[5] J.L. Bear, Y. Li, B. Han, E.V. Caemelbecke, K.M. Kadish, Inorg. Chem. 36 (1997) 5449.
[6] C. Lin, T. Ren, E.J. Valente, J.D. Zubkowski, J. Chem. Soc. Dalton Trans. (1998) 571.
[7] C. Lin, T. Ren, E.J. Valente, J.D. Zubkowski, J. Organomet. Chem. 579 (1999) 114.
[8] T.W. Greene, Protective Groups in Organic Synthesis, Wiley, New York, 1981.
[9] A.R. Chakravarty, F.A. Cotton, D.A. Tocher, Inorg. Chem. 24 (1985) 172.
[10] (a) M.P. Doyle, V. Bagheri, T.J. Wandless, N.K. Harn, D.A. Brinker, C.T. Eagle, K.-L. Loh, J. Am. Chem. Soc. 112 (1990) 1906. (b) M.P. Doyle, W.R. Winchester, J.A.A. Hoorn, V. Lynn, S.H. Simonsen, R. Ghosh, J. Am. Chem. Soc. 115 (1993) 9968.
[11] J. Manna, K.D. John, M.D. Hopkins, Adv. Organomet. Chem. 38 (1995) 79 and the earlier Refs. therein.
[12] F.A. Cotton, T. Ren, Inorg. Chem. 34 (1995) 3190.
[13] C. Lin, T. Ren, E.J. Valente, J.D. Zubkowski, E.T. Smith, Chem. Lett. (1997) 753.
[14] R.O. Loutfy, R.O. Loutfy, Can. J. Chem. 54 (1976) 1454.
[15] T. Ren, Coord. Chem. Rev. 175 (1998) 43.
[16] J.G. Osteryoung, R.A. Osteryoung, Anal. Chem. 57 (1985) 101A.
[17] A.R. Chakravarty, F.A. Cotton, D.A. Tocher, J.H. Tocher, Polyhedron 4 (1985) 1475.
[18] T.A. Stephenson, G. Wilkinson, J. Inorg. Nucl. Chem. 28 (1966) 2285.
[19] SAINT V 6.035 Software for the CCD Detector System, Bruker-AXS Inc., 1999.
[20] G.M. Sheldrick, SHELXS-90, Program for the Solution of Crystal Structures, University of Göttingen, Germany, 1990.
[21] G.M. Sheldrick, SHELXL-93, Program for the Refinement of Crystal Structures, University of Göttingen, Germany, 1993.
[22] SHELXTL 5.03 (WINDOW-NT Version), Program Library for Structure Solution and Molecular Graphics, Bruker-AXS Inc., 1998.